Kurdistan Journal of Applied Research (KJAR)
Print-ISSN: 2411-7684 | Electronic-ISSN: 2411-7706

Original Article

Development and Fabrication of Zavegepant Loaded Mucoadhesive Microemulsion for Intranasal Delivery

Akshay C. Vikhe [a], Rahul K. Godge [a]*, Ganesh S. Shinde [b], Dattaprasad N. Vikhe [c], Shubham B. Mhaske [a]

[a] Department of Pharmaceutical Quality Assurance, Pravara Rural College of Pharmacy, Maharashtra, India.
[b] Department of Pharmaceutics, Institute of Pharmacy, Maharashtra, India.
[c] Department of Pharmacognosy, Pravara Rural College of Pharmacy, Maharashtra, India.

Submitted: 20 October 2025
Revised: 09 December 2025
Accepted: 05 January 2026

* **Corresponding Author**: rahulgodge@gmail.com

Keywords: Intranasal delivery, Zavegepant, Response surface methodology, Mucoadhesive, Migraine therapy, Quality-by-design, Optimization.

How to cite this paper: A. C. Vikhe, R. K. Godge, G. S. Shinde, D. N. Vikhe, S. B. Mhaske, "Development and Fabrication of Zavegepant Loaded Mucoadhesive Microemulsion for Intranasal Delivery", KJAR, vol. 11, no. 1, pp: 1-21, Jun 2026, doi: 10.24017/science.2026.1.1

Abstract: To develop and optimize zavegepant-loaded mucoadhesive microemulsions for intranasal delivery, utilizing quality-by-design principles for enhanced bioavailability and rapid onset in acute migraine management. Zavegepant-loaded microemulsions were formulated using Labrafil M 1944 CS (oil), Brij 35 (surfactant), polyethylene glycol (PEG) 400 (co-surfactant), gellan gum (mucoadhesive polymer), and double distilled water. A central composite design with 4 factors (oil, surfactant, co-surfactant, and water concentrations) was employed to optimize critical quality attributes including globule size, zeta potential, and polydispersity index. Comprehensive characterization included particle size analysis, surface charge determination, drug content, permeation studies, and accelerated stability testing. Twenty-seven formulations were evaluated, with statistical analysis identifying concentration as the primary determinant of microemulsion properties (F-values: 144.64-375.27). Optimization yielded formulation (10% Labrafil M 1944 CS, 52% Brij 35, 18% PEG 400, 20% water) with ideal characteristics: globule size 58.7 nm, Polydispersity index 0.142, zeta potential -12.7± mV, and drug content 99.6. It demonstrated superior *ex-vivo* drug permeation (91.7% at 12h) and remained stable for 6 months under accelerated conditions. The optimized mucoadhesive microemulsion showed good *in vitro* results with fast drug release, strong permeation, and stable performance. This suggests it could be a useful intranasal system for zavegepant in treating migraines, but *in vivo* studies are still needed to confirm its clinical use.

1. Introduction

Migraines impose a substantial burden on patients and healthcare systems due to their high prevalence, disabling symptoms, and the limitations of existing therapies, which often provide incomplete relief or are associated with tolerability issues. Zavegepant, a third-generation calcitonin gene-related peptide (CGRP) receptor antagonist, offers distinct advantages including rapid onset of action, favourable safety profile, and efficacy in patients who may not respond well to triptans or oral medications. The rationale for developing an intranasal mucoadhesive microemulsion formulation of Zavegepant lies in its ability to bypass gastrointestinal absorption, ensure faster drug delivery through the nasal mucosa, and enhance bioavailability while minimizing systemic side effects, thereby addressing unmet needs in acute migraine management. Global statistics reveal that migraines affect nearly 1.2 billion people worldwide, ranking as the second leading cause of disability. This widespread condition significantly undermines both quality of life and work productivity, highlighting its profound social and economic consequences [1]. In America, migraine-related fiscal costs are

not inconsiderable and reach more than $ US 78 billion annually due to health costs, lost workdays and reduced productivity at work. When it comes to current migraine therapy, oral medications are the mainstay, but they are plagued by such problems as poor bioavailability and delayed onset, as well as gastrointestinal upset during migraine attacks [2]. Most medications for mouth pain deliver limited relief, often forcing patients to consume larger doses and exposing them to increased risks of side effects [3]. Results from studies indicate a rapidly rising prevalence of migraines, especially in young adults and women and hence the need for developing effective treatment approaches which will leave the patient symptom-free in no time and which will cause minimal systemic side effects [4]. The creation of novel pharmacological agents targeting unique migraine pathophysiology has proven to have a vast potential to promote the development of more effective tools to address these unmet medical demands [5].

Zavegepant has been approved by the United State food and drug administration as an intranasal spray for the acute treatment of migraine in adults. [6]. The intranasal formulation of zavegepant provides rapid therapeutic response within 15 – 30 minutes that demonstrates improved bioavailability as against oral formulation [7]. Through competitive antagonism of CGRP receptors within the trigeminal ganglia and brainstem nuclei, Zavegepant disrupts the inflammatory sequence critical to migraine pathophysiology [8]. Research on zavegepant has confirmed its superior efficacy in treating acute migraine, while demonstrating minimal systemic absorption. This pharmacological profile suggests a potential advantage in reducing the cardiovascular adverse effects commonly associated with established triptan medications and studies on zavegepant suggest it is effective in treating acute migraine with limited systemic absorption. This property may reduce the risk of cardiovascular side effects often linked to triptan medications. However, further clinical evidence is needed to fully establish these advantages [9, 10]. The objective of this study is to develop and optimize a mucoadhesive microemulsion of Zavegepant that is targeted specifically for nasal delivery and which demonstrated both rapid efficacy and enhanced bioavailability as compared to existing oral forms of the product. Important objectives include in-depth examination of surfactant formulations, determination of the most effective mucoadhesive polymer load for enhancing nasal dwell, and strong assessment of physicochemical tests of *in vitro* drug passage through simulated nasal mucosal surfaces will be performed *in vitro*. The targeted achievements are a stable, biocompatible microemulsion, superior to existing standards in pharmacokinetics and therapeutic action and thus capable of overturning current acute migraine prescriptions [11-13].

2. Materials and Methods

2.1. Materials

Zavegepant (pharmaceutical grade, purity >99%) was procured from Sciquaint Innovations (Pune, India); Labrafil M 1944 CS (pharmaceutical grade, medium-chain triglyceride) from Gatte fosse (Mumbai, India); Brij 35 (pharmaceutical grade, HLB 16.9) and Polyethylene Glycol (PEG) 400 (pharmaceutical grade, Molecular weight 380-420 Dalton) from Neeta Chemicals (Pune, India); Gellan gum (pharmaceutical grade, low acyl) from Sciquaint Chemicals (Pune, India); Methanol (HPLC grade, ≥99.9%) and Potassium bromide (IR grade, ≥99%) from Merck Life Science (Mumbai, India); Goat nasal mucosa was freshly obtained from a local slaughterhouse (Pune, India); Dialysis membrane (MWCO 12,000-14,000 Da) from HI Media Laboratories (Mumbai, India). All other chemicals and reagents used were of analytical grade and obtained from standard laboratory suppliers.

2.2. Methods

2.2.1. Calibration Curve of Zavegepant

To determine drug concentration, a calibration curve was obtained for Zavegepant using Ultraviolet (UV) spectrophotometric methods. The stock solution of zavegepant of 1000 μg/mL was prepared by dissolving 10 mg of the compound in 10 mL pure methanol. A set of dilutions was performed using double distilled water in order to provide a range of concentrations of 10-60 μg/mL. Measurement was made by Shimadzu UV-1800 (Kyoto, Japan) UV-Visible spectrophotometry at 280 nm wavelength. Each sample was analysed three times with baseline adjustment to the blank solvent.

Microsoft Excel was used to establish a linear regression equation to ascertain the linearity of data. Results were tabulated in mean ± standard deviation [14-16]. Figure 1 shows calibration curve of zavegepant in methanol.

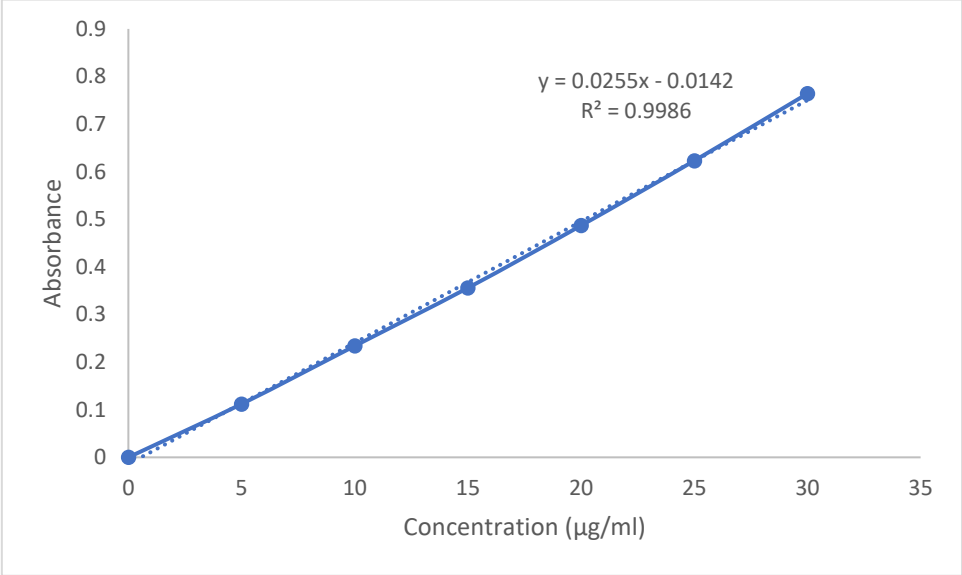

Figure 1: Calibration curve of Zavegepant.

2.2.2. Fourier Transform Infrared Spectroscopy Analysis

Study of functional groups and assessment of drug-excipient interactions was done using Fourier Transform Infrared spectroscopy. In combination, 5 mg Zavegepant, each of the individual excipients, and the physical mixture were mixed with 100 mg of potassium bromide in the infrared grade powder. Thin pellets were obtained through the application of 10 tons pressure 2 minutes to the mixture with the aid of Specac Hydraulic press. Transmission mode Fourier-transform infrared spectroscopy (FTIR) spectra were acquired utilizing Bruker Alpha II FTIR spectrometer (Bruker, Massachusetts, USA) for the samples. Fourier transform spectra were obtained throughout the wavenumber region 4000-400 cm^{-1} at a resolution of 4 cm^{-1} and each sample was scanned 32 times. In order to remove background noise, the measurements were made with blank KBr pellets. All analyses were performed under ambient conditions: at 25 ± 2°C, with a minimum of triplicate applied to the samples [17].

2.2.3. Differential Scanning Calorimetry Analysis

Differential Scanning Calorimetry was used to study thermal behaviour and compatibility of Zavegepant and excipients. Each sample (Zavegepant, individual excipients, and the physical mixture) was weighed accurately in 5-8 mg and sealed in aluminium pans. The analysis received from differential scanning calorimetry (DSC) 214 Polyma of Netzsch, Germany under a nitrogen gas of 50ml/min flow at a heating rate of 10°C/min as the samples was heated at a range of 30°C to 300°C. The reference sample was an empty aluminium pan. To analyze and report the onset temperature, peak temperature and enthalpy change (ΔH), the Proteus analysis software was used. The samples were measured thrice [18].

2.2.4. Solubility Studies in Different Oils

Solubility of Zavegepant was determined based on the guidelines provided by USP, following a shake-flask method. An excess quantity of Zavegepant was introduced into 5 ml of several types of oils (Labrafil M 1944 CS, Capryol 90, Oleic acid), found in amber screw-capped vials. After 2 mins vortexing, they were incubated in a thermostatically controlled water bath (Julabo SW23, Germany) at 37 ± 0.5°C for a period of 72 hours, under shaking condition 100 rpm. Samples were separated using a centrifuge (Remi R-24, India) by centrifuging at 3000 rpm for 10 mins. The supernatant was diluted with methanol through an appropriate method. Quantification of drug concentration was achieved by

means of spectrophotometric analysis at 280 nm. Solubility was determined in mg/mL and each experiment was performed three times in triplicate [19, 20].

2.2.5. Ternary Phase Diagram Construction

The boundaries of microemulsion regions were defined using phase diagrams obtained from water titration. Solution samples were formed with a 1:1, 2:1 and 3:1 ratio of surface active agent and co – surface active agent. A couple of blends consisting of Labrafil M 1944 CS oil and Smix were made in 5 ml glass vials, each ratio 1:9 to 9:1. Dropwise addition of double distilled water, followed by vigorous vortexing was maintained until mixture clouded or separated in phases. Phase separation or turbidity was conspicuous, and water concentration was recorded at this stage. Staining and isotropy of the samples were established by examining them with ordinary and polarized light. A Web server (https://ternaryplot.com/) was used to generate phase diagrams with oil, Smix, and water used as the three axes. The microemulsion zones were identified by the clear, transparent and uniformly isotropic areas [21, 22].

2.2.6. Experimental Design

Central Composite Design (CCD) was employed to optimize formulation variables, like globule size, zeta potential, and polydispersity index. The objective was to minimize globule size and polydispersity index, while simultaneously maximizing zeta potential. To achieve this, the study examined dependent variables such as viscosity, particle size, and dissolution rate, in relation to independent variables including the concentration of ingredients and polymers. By conducting a limited number of experiments, CCD enabled high validity in modeling curvature trends and interactions among factors and responses. Using Design Expert software (Stat-Ease, USA) to guide the experimental design, a 4-factor, 5-level Central Composite Design was used. The formulation factors were as follows Labrafil M 1944 CS (10-20% v/v), Brij 35 (38-52% v/v), PEG 400 (12-18% v/v). Twenty-seven of experimental runs were carried out including points of factorials, axial points, and center points. The design equation was:

$$Y = \beta_0 + \beta_1X_1 + \beta_2X_2 + \beta_3X_3 + \beta_4X_4 + \beta_{12}X_1X_2 + \beta_{13}X_1X_3 + \beta_{14}X_1X_4 + \beta_{23}X_2X_3 + \beta_{24}X_2X_4 + \beta_{34}X_3X_4 + \beta_{11}X_1^2 + \beta_{22}X_2^2 + \beta_{33}X_3^2 + \beta_{44}X_4^2$$

where Y represents the response variable, β represents regression coefficients, and X_1, X_2, X_3, X_4 represent independent variables. Response variables measured were globule size (nm), zeta potential (mV), and polydispersity index (PDI). Table 1 shows independent variables and response variables for CCD and table 2 shows formulation composition.

Table 1: Independent variables and response variables for central composite design.

Sr. No.	Independent Variables	Levels (%v/v)				
		Low (-1)	Medium (0)	High (+1)	-α	+α
1.	Labrafil M 1944 CS	10	15	20	5	25
2.	Brij 35	38	45	52	31	59
3.	PEG 400	12	15	18	9	21
4.	Double distilled water	20	25	30	15	35
	Response Variable	**Unit**	**Goal**			
Y^1	Globule Size	nm	Minimize			
Y^2	Zeta Potential	mV	Maximize			
Y^3	Polydispersity Index (PDI)	-	Minimize			

Table 2: Formulation composition for dental composite design.

Run	Labrafil M 1944 CS (%v/v)	Brij 35 (%v/v)	PEG 400 (%v/v)	DDW (%v/v)	Gellan gum (%w/v)	Zavegepant (mg)
A1	10	52	12	30	0.1	200
A2	15	45	15	25	0.1	200
A3	15	59	15	25	0.1	200
A4	15	45	15	35	0.1	200
A5	20	52	12	20	0.1	200
A6	10	38	12	30	0.1	200
A7	20	52	18	20	0.1	200
A8	20	38	18	30	0.1	200
A9	10	52	18	30	0.1	200
A10	25	45	15	25	0.1	200
A11	15	45	21	25	0.1	200
A12	20	52	18	30	0.1	200
A13	10	52	12	20	0.1	200
A14	15	45	15	25	0.1	200
A15	10	38	12	20	0.1	200
A16	20	38	12	20	0.1	200
A17	10	52	18	20	0.1	200
A18	20	52	12	30	0.1	200
A19	15	31	15	25	0.1	200
A20	15	45	15	25	0.1	200
A21	15	45	15	15	0.1	200
A22	5	45	15	25	0.1	200
A23	10	38	18	30	0.1	200
A24	10	38	18	20	0.1	200
A25	20	38	18	20	0.1	200
A26	20	38	12	30	0.1	200
A27	15	45	9	25	0.1	200

2.2.7. Preparation of Microemulsion

The CCD design applied to prepare microemulsion formulations through the spontaneous emulsification approach. The oil phase containing the Labrafil M 1944 CS was admixed with the surfactant at 300 rpm with magnetic stirring (Remi 2MLH, India) for 5 mins. For 5 more mins, mixing was carried out following the addition of the co-surfactant. Once clear and transparent microemulsion was formed it was retrieved by adding a double distilled water drop by drop with stirring at 500 rpm until the desired clarity was achieved. The microemulsions were then each vigorously mixed for 15 mins to ensure the optimal equilibrium was achieved. Zavegepant was incorporated in the emulsion whereby it was incorporated in the oil phase; this was before the mixing started. The preparations were performed under room temperature (25 ± 2^0C) and the final formulations were stored in amber glass vials protected from light [23, 24].

2.2.8. Characterization of Mucoadhesive Microemulsion

2.2.8.1. Visual Inspection

Visual examination was employed to evaluate the important aspects of the physical appearance, transparency, and uniformity in the microemulsion formulations. Visual inspection was performed using usual light with white and black backgrounds to evaluate the degree of transmittance and opalescence of each preparation. To determine if the samples are isotropic, each was observed at 100× magnification under polarized light on a polarizing microscope (Labomed CxL, Mumbai, India). Phase separation, precipitation or turbidity was recorded. All the observations were documented at ambient temperature (25 ±2°C) and verified through the use of digital pictures. Three replicates samples of each formulation were made and examined immediately after preparation ad after 24 hours [25].

2.2.8.2. Globule Size Determination

Globule size analysis was performed *in vitro* by using dynamic light scattering (DLS) method through the use of Zetasizer Nano ZS apparatus, through Malvern Panalytical Pune, India. To achieve the best scattering intensity, samples were diluted in a 1:100 ratio with double distilled filtered water. Measurements were carried out at a temperature of 25 °C and a 2minute equilibration interval. The refractive index was adjusted at 1.330 for aqueous solvent; 1.450 for the dispersed substance. Samples were analyzed five times, using the instrument's automatic mode of measurement. The results were presented as the mean globule diameter (Z - average) and standard deviation. The parameters of each formulation were determined three separate times [26].

2.2.8.3. Polydispersity Index Measurement

Measuring polydispersity index in tandem with globule size was performed on Zetasizer Nano ZS from Malvern Panalytical in Pune, India. The PDI value which determines the dispersion in the size distribution was calculated by the instrument software using the cumulants analysis method. The samples were prepared and analysed according to the same protocol as used when measuring globule size. The value of PDI below 0.3 was employed to verify a narrow size distribution. Each sample was analysed in triplicate and the duplicates obtained were averaged in five replicates [27].

2.2.8.4. Zeta Potential Determination

By using Zetasizer Nano ZS (Malvern Panalytical, Pune, India), provided with laser Doppler electrophoresis, Zeta potential measurements were carried out. The samples were diluted a 1:100 dilution with filtered double distilled water before being introduced into universal dip cells. The measurements were made at 25°C using the Smoluchowski approximation application. The sample was taken with a voltage = 5V and a duration set automatically by the conductivity of the solution. The acquired data were in millivolts (mV) with their standard deviation proper. Ten analyses were performed on three different samples [28].

2.2.8.5. pH Determination

pH determinations were done using a digital pH meter (Systronics μpH System 361, Hyderabad, India, with calibrations with buffer solutions of pH 4.0, 7.0, and 9.2. The electrode pH was directly inserted into microemulsion sample at ambient temperature (25 ± 2°C). Preliminary pH readings have settled down after 2 minutes equilibration of the samples. Each of the formulations was tried thrice in order to give accuracy, and measurements were recorded to ±0.01 pH units [29].

2.2.8.6. Determination of Mucoadhesive strength

Mucoadhesive strength was determined using a modified weight balance method with fresh goat nasal mucosa obtained from a local slaughterhouse (Pune, India). The mucosal tissue was carefully cleaned with phosphate buffer (pH 6.8) and cut into uniform pieces (2×2 cm). Two circular glass slides (diameter 2.5 cm) were used, with the lower slide having the mucosal tissue attached using cyanoacrylate adhesive, keeping the mucosal surface upward. A fixed volume (0.5 mL) of microemulsion was applied to the tissue surface and allowed to hydrate for 2 minutes. The upper slide was then gently placed on the hydrated tissue and maintained in contact for 1 min under a constant pressure of 0.5 N. The assembly was attached to a modified weight balance, and weights were gradually added to the right pan until detachment occurred. The mucoadhesive strength was calculated as the minimum weight required for detachment and expressed in Newtons (N). Each formulation was analysed in triplicate at ambient temperature (25 ± 2°C), and results were presented as mean ± standard deviation [30].

2.2.8.7. Viscosity Measurement

Viscosity measurement in low viscosity samples was carried out using Brookfield DV-II+ Pro viscometer (Brookfield, Mumbai, India), with the use of spindle 64. The viscometry was performed at a frequency of 100 rpm with samples held at 25 ± 1°C. Measurements were done using a small sample adapter with 7ml sample. Data were recorded after 60 seconds of the motor running at full steadiness. Measurement outcomes were presented in centipoise (cP) as viscosity. All samples were subjected to a triplicate analysis and the mean values were presented [31].

2.2.8.8. Drug Content Determination

The assay for drug content was evaluated using UV spectrophotometry on equipment supplied by Systronics 2203, manufactured in Hyderabad India. Samples of microemulsions were diluted 10-fold with methanol and centrifuged at 3000 rpm for ten minutes. Filtering 0.45 μm membrane filter supernatant, it was diluted further with a phosphate buffer pH 6.8. UV spectrophotometer was used to measure assay absorbance at 280 nm after a calibration was done. The amount of the drug present was defined from the linear calibration curve ($y = 0.0548x + 0.0265$, $r^2 = 0.999$), and the result was presented in percentage using three Independent samples [32].

2.2.8.9. Permeation Study Through Nasal Mucosa

Ex vivo permeation studies were conducted using the Franz diffusion cells from Orchid Scientific from Nashik, India, with a useful diffusion area of 1.77 cm^2 and a receptor volume of 15ml. Goat nasal mucosa was harvested and washed with phosphate buffer at pH 6.8, cut to the appropriate dimensions, and placed in the diffusion cell with the epithelial surface facing the donor chamber and the submucosal/connective tissue side facing the receptor chamber. The phosphate buffer pH 6.8 was saturated with 0.1% sodium lauryl sulphate as penetration in the receptor compartment. At time zero, 0.5 ml microemulsion was applied to the surface of mucosa. At fixed time points (0.5, 1, 2, 4, 6, 8, 10 and 12 hours), samples of 1 ml were taken and the receptor compartment was replenished with the same volume (1 mL) of fresh buffer. The drug diffusing was measured with the UV spectrophotometer at the wavelength of 280 nm. Based on the provided equations, cumulative diffusion (μg/cm^2), steady-state flux (Jss, μg/cm^2/h), permeability coefficient (Kp, cm/h), lag time (TL, h), and enhancement ratio compared to control were calculated. Jss represents the slope of the linear part of the drug permeated accumulated versus time plot; Kp is represented by Jss/Cd; TL is defined as the x intercept of the linear fraction of the data set. The measurements were taken as duplicate samples for each experiment, all samples taken from the same source of tissue [33, 34].

2.2.9. Stability Studies

The accelerated stability studies were planned in accordance to the International Conference on Harmonization (ICH) guidelines Q1A (R2). Stability chambers from Thermolab, Mumbai, India were utilised to store sealed microemulsion samples at 40 ± 2°C/75 ± 5% relative humidity (RH). Samples taken at months 0, 1, 2, 3 and 6 were subjected to physical appearance, pH, globule size, PDI, zeta potential, drug content and microbial growth. Simultaneously, stability analyses at 25 ± 2°C/60 ± 5% RH were conducted for the long term. Statistical analysis of the changes from initial values was done to determine changes. Six batch samples were screened at each sampling interval for each of the three batches [35].

2.2.10. Morphological Analysis

The transmission electron microscopy examination was conducted by using JEM-2100 (JEOL, Delhi, India) at the accelerating voltage of 120 kV. To achieve sample preparation the microemulsions were diluted 1:50 in filtrated water, and applied to the carbon-coated copper grids. The method of negative staining was to immerse the samples in a 2% aqueous uranyl acetate solution. After preparing the samples they were dried at room temperature for analysis. Micrographs were captured with magnifications ranging from 5000× to 50000× to determine globular form and particle size. Three viewing fields were analysed and representative images were carefully selected [36, 37].

2.2.11. Statistical Analysis

The mean ± standard deviation is used to present each set of experimental data. In all statistical evaluations, GraphPad Prism 8.0 software (GraphPad Software Inc., San Diego) was used. For group means comparisons, a one-way ANOVA was conducted. To compare the individual groups, a student's t-test was used. Using Design Expert software (Version 13, Stat-Ease Inc.) the response surface methodology and regression analysis were carried out. If p values were below 0.05, all analyses were considered as statistically significant.

3. Results

3.1. Differential Scanning Calorimetry Analysis

Zavegepant's melting point was identified in the DSC analysis by a characteristic endothermic peak that manifested at 198.11°C as shown in figure 2A. Two physical mixture peaks were observed (Figure 2B) at 118.33°C and 198.75°C, which indicate that the components have separated. The Preliminary stability data indicate that the formulation shows potential for commercialization, though longer-term studies are required to confirm its shelf-life and robustness under varied storage conditions. DSC Spectra of zavegepant at 198.11ºC and physical mixture at 118.33 and 198.75 ºC shown in figure 2.

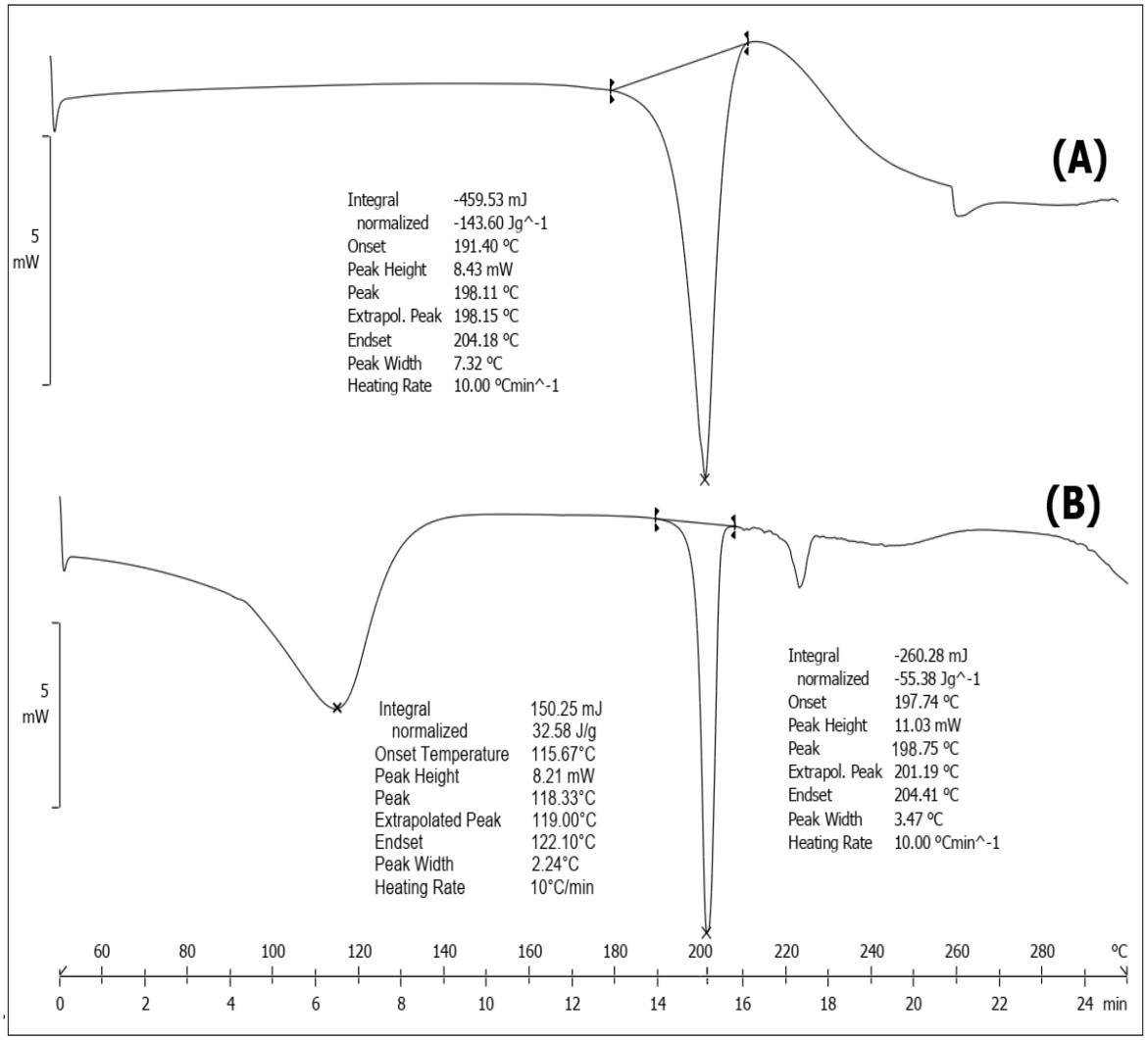

Figure 2: Differential Scanning Calorimetry thermograms showing (A) pure zavegepant, which exhibits a sharp endothermic peak corresponding to its melting point at 198.11 °C, and (B) the physical mixture of zavegepant with excipients, displaying two distinct endothermic transitions at 118.33 °C (attributed to the excipient component) and 198.75 °C of Zavegepant.

3.2. Fourier Transform Infrared Spectroscopy Analysis

The FTIR spectrum of Zavegepant showed characteristic peaks at 3143.08 cm $^{-1}$ (N-H stretch), 2943.90 cm $^{-1}$ (C-H stretch), 1 Physical mixture showed its peaks at 3801.54 cm^{-1}, 2969.80 cm^{-1}, 1700.14 cm^{-1} and 1011.17 cm^{-1}; these were shifted slightly from Zavegepant Observed peaks formed in the drug and that of the physical mixture were identical, affirming no new formation resulting no loss confirming the compatibility of Zavegepant with excipients and lack of a chemical interaction. FTIR spectra of (A) pure Zavegepant and (B) its physical mixture with excipients shown in figure 3.

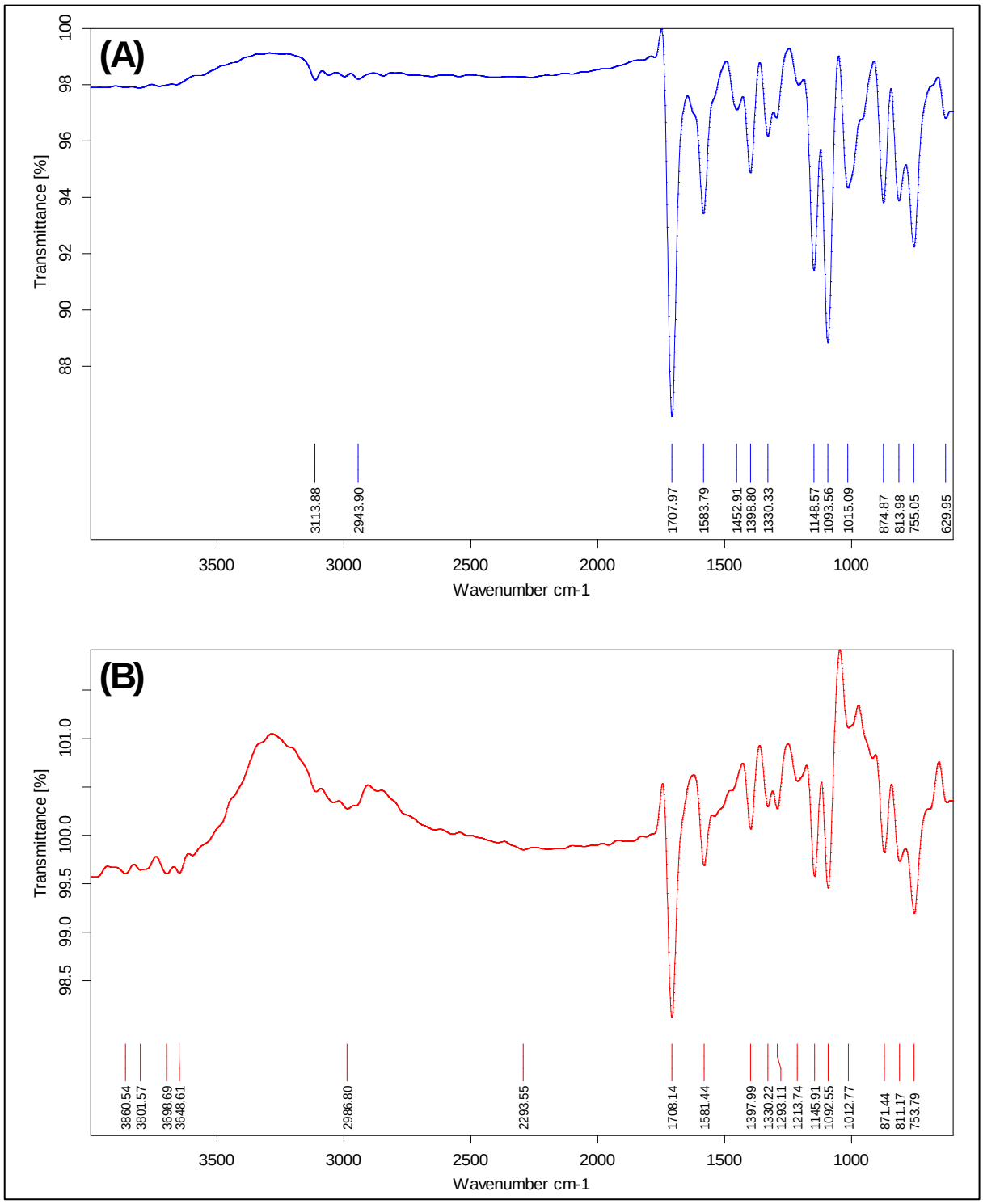

Figure 3: Fourier Transform Infrared spectra of (A) pure zavegepant and (B) its physical mixture with excipients.

3.3. Zavegepant Solubility in Different Oils

Through assessment of Zavegepant solubility in various oils, the optimal oil phase for micro-emulsion assembly was defined. The results showed that Labrafil M 1944 CS (Oleoyl polyoxyl-6 glycerides**)** was the most solubilized for the drug (47.86 ± 2.31 mg/mL) with Transcutol HP in second position (34.52 ± 1.13 mg/mL) By comparison, the minimum solubility in Castor oil was measured at 12.38 ± 0.87 mg/mL. The higher observed solubility in Labrafil M 1944 CS was attributed to its medium-chain triglyceride structure and amphiphilic nature, which facilitated desirable hydrogen bond-

ing with the drug. Labrafil M 1944 CS was determined by these results to be the best oil phase to use for future preparations of microemulsions.

3.4. Ternary Phase Diagram

The water titration method was used to obtain ternary phase diagrams; thus, we were able to find the microemulsion regions with the various Smax ratios. The 3:1 surfactant to co-surfactant (PEG 400) ratio produced the widest microemulsion range, covering approximately 42% of the area, compared to a 28% and 19% for ratios of 2. The greater size of the microemulsion zone at 3:1 ratio demonstrated a better HLB distribution and stronger interfacial film stability, thus making more flexible formulation design possible. In addition, the 3:1 ratio produced clear, transparent microemulsions over a broader range of oil and water compositions validating its use in the formulation of the best microemulsion. Ternary phase diagrams showing microemulsion regions at different surfactant ratios shown in figure 4.

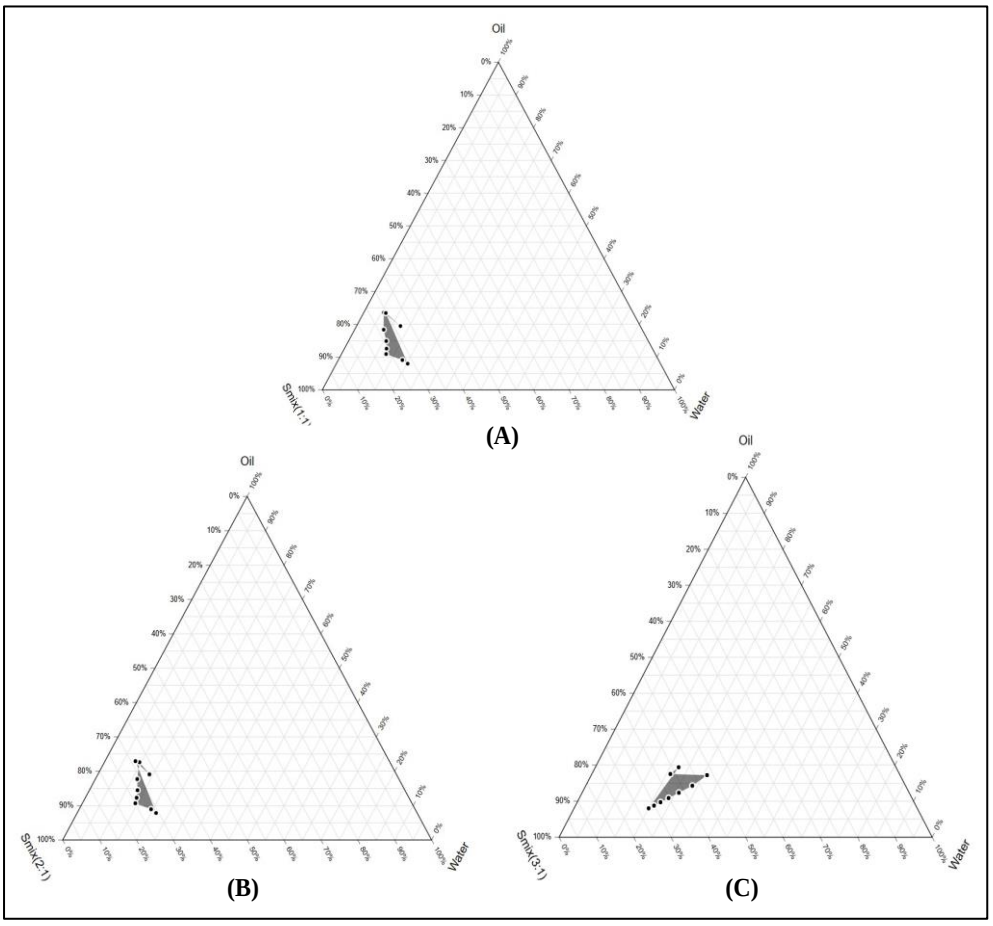

Figure 4: Ternary phase diagrams showing microemulsion regions at different surfactant ratios. (A) 1:1 ratio of Brij 35 and PEG 400, (B) 2:1 and PEG 400, (C) 3:1 ratio and PEG 400. Shaded areas represent microemulsion regions, with oil (Labrafil M 1944 CS), surfactant-co-surfactant mixture (Smix), and water at the three corners.

3.5. Characterization of Zavegepant-Loaded Microemulsions

Zavegepant-loaded microemulsions are characterized by their nanoscale droplet size, stability, and ability to enhance drug solubility and bioavailability. These systems typically exhibit globule sizes in the nanometer range with low polydispersity index, ensuring uniform distribution, while negative zeta potential values contribute to electrostatic stabilization. Table 3 summarizes the visual stability evaluation of 27 formulation batches. Clear, transparent, and colorless samples without phase separation (AF1–AF3, AF7, AF9, AF12–AF14, AF17, AF20–AF22) indicate stable formulations, while turbid, opaque, or milky batches with partial/major separation (AF5, AF10, AF16, AF19, AF25, AF26)

show instability. Slightly turbid or semi-transparent batches without separation represent borderline stability.

Table 3: Physical inspection results showing macroscopic appearance, transparency, color and phase separation.

Batch	Appearance	Transparency	Color	Phase Separation
AF1	Clear	Transparent	Colorless	None
AF2	Clear	Transparent	Colorless	None
AF3	Clear	Transparent	Colorless	None
AF4	Slightly Turbid	Semi-transparent	Slightly milky	None
AF5	Turbid	Opaque	Milky white	Partial
AF6	Turbid	Translucent	White	Minor
AF7	Clear	Transparent	Colorless	None
AF8	Highly Turbid	Opaque	White	Partial
AF9	Clear	Transparent	Colorless	None
AF10	Turbid	Opaque	Milky white	Major
AF11	Clear to Turbid	Semi-transparent	Slightly cloudy	None
AF12	Clear	Transparent	Colorless	None
AF13	Clear	Transparent	Colorless	None
AF14	Clear	Transparent	Colorless	None
AF15	Slightly Turbid	Translucent	Whitish	None
AF16	Turbid	Opaque	Milky white	Partial
AF17	Clear	Transparent	Colorless	None
AF18	Turbid	Translucent	White	Minor
AF19	Highly Turbid	Opaque	White	Major
AF20	Clear	Transparent	Colorless	None
AF21	Clear	Transparent	Colorless	None
AF22	Clear	Transparent	Colorless	None
AF23	Turbid	Translucent	Whitish	Minor
AF24	Slightly Turbid	Semi-transparent	Cloudy	None
AF25	Turbid	Opaque	Milky white	Partial
AF26	Highly Turbid	Opaque	White	Major
AF27	Slightly Turbid	Semi-transparent	Slightly hazy	None

Physicochemical parameters such as pH, viscosity, and mucoadhesive strength are measured to confirm suitability for intranasal or oral delivery, maintaining near-neutral pH and moderate viscosity for patient comfort and effective mucosal adhesion. The table 4 summarizes the physicochemical evaluation of 27 batches, showing that all formulations maintained consistent properties within acceptable ranges. The mean globule size was 106.2 nm with moderate variability, zeta potential averaged –19.4 mV indicating sufficient electrostatic stability, and polydispersity index (0.29) reflected good uniformity of particle distribution. The pH remained near neutral (6.41), viscosity averaged 86.4 cP suggesting moderate flow behavior, mucoadhesive strength was 0.65 N indicating good adhesion, and drug content was consistently high (~98.8%). Although some batches showed extremes (e.g., AF22 with the smallest size and highest drug content, AF19 with the largest size and strongest adhesion), the ANOVA p-values for all parameters were greater than 0.05, confirming that differences among batches were statistically non-significant. This demonstrates reproducibility and robustness of the formulation process, ensuring stable quality and performance across all batches despite minor variations. Figure 5 shows optimization of Zavegepant microemulsion batches via central composite design.

Table 4: Characteristics of zavegepant-loaded microemulsions prepared using CCD.

Batch	Globule Size (nm) ± SD	Zeta Potential (mV) ± SD	PDI ± SD	pH ± SD	Viscosity (cP) ± SD	Mucoadhesive Strength (N) ± SD	Drug Content (%) ± SD
AF1	78.5 ± 3.2	-12.4 ± 0.8	0.192 ± 0.025	6.42 ± 0.08	52.4 ± 3.1	0.47 ± 0.03	98.7 ± 1.2
AF2	92.1 ± 4.1	-18.7 ± 1.2	0.245 ± 0.031	6.38 ± 0.06	74.2 ± 4.5	0.58 ± 0.04	99.1 ± 1.0
AF3	68.4 ± 2.8	-14.2 ± 0.9	0.168 ± 0.021	6.45 ± 0.07	48.6 ± 2.8	0.42 ± 0.03	99.4 ± 0.9
AF4	105.2 ± 5.3	-22.1 ± 1.5	0.287 ± 0.038	6.35 ± 0.09	83.7 ± 5.2	0.64 ± 0.05	98.9 ± 1.1
AF5	114.8 ± 6.2	-15.8 ± 1.1	0.312 ± 0.042	6.51 ± 0.11	95.3 ± 6.8	0.72 ± 0.06	97.6 ± 1.4
AF6	135.7 ± 7.1	-24.5 ± 1.7	0.378 ± 0.045	6.29 ± 0.08	108.2 ± 7.4	0.78 ± 0.07	98.2 ± 1.3
AF7	87.3 ± 3.9	-13.6 ± 0.8	0.213 ± 0.028	6.48 ± 0.07	65.7 ± 4.1	0.52 ± 0.04	99.2 ± 0.8
AF8	152.6 ± 8.4	-27.3 ± 1.9	0.425 ± 0.051	6.32 ± 0.10	124.5 ± 8.9	0.89 ± 0.08	97.8 ± 1.5
AF9	65.2 ± 2.5	-11.8 ± 0.7	0.156 ± 0.019	6.44 ± 0.06	54.3 ± 3.2	0.48 ± 0.03	99.5 ± 0.7
AF10	142.7 ± 7.8	-19.4 ± 1.3	0.395 ± 0.047	6.53 ± 0.12	112.8 ± 8.6	0.83 ± 0.07	96.9 ± 1.6
AF11	98.6 ± 4.5	-17.2 ± 1.1	0.258 ± 0.033	6.41 ± 0.08	78.9 ± 5.0	0.61 ± 0.05	98.8 ± 1.0
AF12	98.3 ± 4.3	-16.9 ± 1.0	0.254 ± 0.032	6.46 ± 0.07	71.4 ± 4.6	0.56 ± 0.04	99.0 ± 0.9
AF13	71.9 ± 3.0	-13.1 ± 0.8	0.175 ± 0.022	6.43 ± 0.08	49.8 ± 2.9	0.45 ± 0.03	99.3 ± 0.8
AF14	93.5 ± 4.0	-18.9 ± 1.2	0.248 ± 0.031	6.39 ± 0.06	75.6 ± 4.8	0.59 ± 0.04	99.2 ± 0.9
AF15	125.4 ± 6.5	-25.8 ± 1.8	0.358 ± 0.043	6.30 ± 0.09	96.7 ± 6.5	0.74 ± 0.06	98.5 ± 1.3
AF16	145.3 ± 7.9	-26.1 ± 1.8	0.412 ± 0.049	6.52 ± 0.11	104.3 ± 7.8	0.79 ± 0.07	97.9 ± 1.4
AF17	58.7 ± 2.1	-12.7 ± 0.8	0.142 ± 0.018	6.47 ± 0.07	58.2 ± 3.5	0.51 ± 0.04	99.6 ± 0.7
AF18	122.4 ± 6.8	-17.5 ± 1.2	0.335 ± 0.041	6.50 ± 0.10	89.5 ± 6.2	0.68 ± 0.05	98.7 ± 1.1
AF19	168.9 ± 9.2	-31.4 ± 2.1	0.485 ± 0.058	6.25 ± 0.12	135.7 ± 9.8	0.94 ± 0.09	97.2 ± 1.7
AF20	94.2 ± 4.1	-19.0 ± 1.2	0.247 ± 0.031	6.37 ± 0.06	74.8 ± 4.7	0.57 ± 0.04	99.1 ± 0.9
AF21	76.8 ± 3.3	-16.2 ± 1.0	0.189 ± 0.024	6.44 ± 0.08	68.3 ± 4.3	0.53 ± 0.04	99.4 ± 0.8
AF22	45.3 ± 1.8	-14.7 ± 0.9	0.118 ± 0.015	6.39 ± 0.07	42.8 ± 2.5	0.38 ± 0.03	99.7 ± 0.6
AF23	132.8 ± 7.0	-23.6 ± 1.6	0.372 ± 0.044	6.31 ± 0.09	105.4 ± 7.6	0.77 ± 0.06	98.4 ± 1.2
AF24	115.2 ± 5.8	-24.9 ± 1.7	0.335 ± 0.041	6.33 ± 0.08	98.2 ± 6.8	0.73 ± 0.06	98.6 ± 1.1
AF25	138.5 ± 7.5	-25.2 ± 1.7	0.388 ± 0.046	6.54 ± 0.11	101.7 ± 7.4	0.76 ± 0.06	98.0 ± 1.3
AF26	158.7 ± 8.7	-28.4 ± 1.9	0.448 ± 0.053	6.49 ± 0.10	118.9 ± 8.5	0.85 ± 0.07	97.7 ± 1.5
AF27	108.4 ± 5.7	-20.3 ± 1.4	0.295 ± 0.037	6.40 ± 0.08	82.1 ± 5.4	0.62 ± 0.05	98.9 ± 1.0
Mean ± SD	106.2 ± 32.4	-19.4 ± 5.5	0.29 ± 0.10	6.41 ± 0.08	86.4 ± 25.1	0.65 ± 0.15	98.8 ± 0.7
ANOVA p-value	0.13^{ns}	0.1^{ns}	0.07^{ns}	0.12^{ns}	0.1^{ns}	0.08^{ns}	0.09^{ns}

ns: non-significant difference.

Figure 5: Zavegepant-loaded microemulsion batches prepared through Central Composite Design, illustrating the systematic optimization of formulation variables to evaluate their influence on globule size, zeta potential, polydispersity index, viscosity, pH, mucoadhesive strength, and drug content.

3.6. Optimization of Zavegepant-Loaded Microemulsions

3.6.1. Effect of Formulation Variables on Globule Size (Y^1)

Statistical analysis showed that quadratic model for globule size was very remarkable ($p < 0.0001$), with adjusted R^2 values 0.9009 and predicted R^2 values 0.7369 (Table 5), highlighting suitability for optimization studies. A value of 17.88 F for the model supported this model for explaining the relationship between formulation variables and globule size. Among the tested factors, concentration (B) showed the highest impact with an F-value of 144.64 ($p < 0.0001$), which was greater than that of Labrafil M 1944 CS (A) with an F-value of 72.09. In comparison, DDW concentration (D) and PEG 400 (C) demonstrated moderate significance, with F-values of 8.10 ($p = 0.0147$) and 5.99 ($p = 0.0308$), respectively. The quadratic effect B^2 showed a high influence (F-value = 13.29, $p = 0.0034$), validating a non-linear relationship between the concentration and the size of the globule. From the analysis, it was clear that the interaction between factors A and B was marginally important (F-value = 2.29, $p = 0.1559$), with all other interactions having little if any significance.

Globule Size = +93.27 + 35.78A - 50.68B - 10.31C + 11.99D + 15.63AB - 6.23AC + 1.28AD - 13.02BC - 5.93BD + 2.83CD + 7.93A^2 + 32.58B^2 + 17.43C^2 + 4.93D^2

The polynomial model revealed that incorporating a quadratic term (B2 – 3.258) significantly enhanced its accuracy, effectively capturing the non-linear behavior of the data. Notably, the smallest globule size was achieved at approximately 52% surfactant and 10% Labrafil M 1944 CS. This outcome highlights the intricate interplay between surfactant and oil concentrations, underscoring the need for precise optimization of these variables to achieve the desired formulation performance.

Table 5: Fit summary of response variables for CCD.

Source	Sequential p-value	Lack of Fit p-value	Adjusted R^2	Predicted R^2	Model Suggested
		Y^1: Globule Size (nm)			
Linear	< 0.0001*	0.0068	0.8578	0.8207	2FI
2FI	0.8257^{ns}	0.0056	0.8334	0.7459	
Quadratic	**0.0341***	**0.0089**	**0.9009**	**0.7369**	✓
Cubic	0.8035 ^{ns}	0.0036	0.8535	-2.2343	Aliased
		Y^2: Zeta Potential (mV)			
Linear	< 0.0001*	0.0064	0.8925	0.8578	2FI
2FI	0.6996 ^{ns}	0.0056	0.8807	0.8432	
Quadratic	**0.0110***	**0.0109**	**0.9423**	**0.8468**	✓
Cubic	0.0625 ^{ns}	0.0254	0.9851	0.6773	Aliased
		Y^3: PDI			
Linear	< 0.0001*	0.0014	0.8590	0.8222	2FI
2FI	0.7035 ^{ns}	0.0012	0.8433	0.7622	
Quadratic	**0.0262***	**0.0021**	**0.9112**	**0.7640**	✓
Cubic	0.7937 ^{ns}	0.0009	0.8707	-1.8620	Aliased

ns: non-significant difference, *: significant difference.

3.6.2. Effect of Formulation variables on Zeta Potential (Y^2)

The quadratic model for zeta potential had impressive statistical accuracy with an adjusted R^2 value of 0.9423 and a predicted R^2. The model exhibited excellent overall performance; in particular concentration (B), which had a very notable F value of 375.27 (p The Labrafil M 1944 CS (A) concentration exhibited a moderate significance with an F-value of 23.16 and with p-value of 0.0004; the DDW concentration on the other. PEG 400 (C) came close to significance, having an F-value of 4.47 and p-value of 0.0560. Among the quadratic terms, B^2 was highly remarkable (F-value = 13.84, p = 0.0029) suggesting non-linear effects were present. The AD interaction term was moderately remarkable (F-value = 6.52, p = 0.0253), but no other interaction term was statistically remarkable. A major lack of fit in the model (p=0.0109) suggests the presence of other factors beneath the ones mentioned.

Zeta Potential = -18.87 - 2.62A + 10.53B + 1.15C - 1.42D - 1.40AB + 0.50AC - 3.40AD + 0.00BC - 0.40BD - 0.30CD + 1.46A^2 - 4.29B^2 - 0.24C^2 - 0.64D^2

The strong negative coefficient of -4.29 on the quadratic term (B^2) indicated the presence of a peaked response curve. In addition, a clear negative interaction coefficient (-3.40) for the AD pair suggested that higher levels of oil and water suppress the achievement of an optimal surface charge. Overall, the results demonstrated that the maximum zeta potential is attained at a balance between intermediate ranges of the formulation variables, highlighting the importance of fine-tuning these factors for stability. Table 6 shows fit summary of response variables for CCD and ANOVA summary for quadratic models of all responses.

Table 6: ANOVA summary for quadratic models of all responses.

Source	Sum of Squares	df	Mean Square	F-value	p-value
Model	26671.75	14	1905.12	17.88	< 0.0001*
A-Labrafil M 1944 CS	7679.10	1	7679.10	72.09	< 0.0001*
B-Brij 35	15407.73	1	15407.73	144.64	< 0.0001*
C-PEG 400	637.57	1	637.57	5.99	0.0308*
D-DDW	862.80	1	862.80	8.10	0.0147*
AB	244.14	1	244.14	2.29	0.1559^{ns}
AC	38.75	1	38.75	0.36	0.5576^{ns}
AD	1.63	1	1.63	0.02	0.9037^{ns}
BC	169.65	1	169.65	1.59	0.2309^{ns}
BD	35.11	1	35.11	0.33	0.5765^{ns}
CD	7.98	1	7.98	0.07	0.7890^{ns}
A^2	83.83	1	83.83	0.79	0.3925^{ns}

Table 6: Continue.

B^2	1415.20	1	1415.20	13.29	0.0034*
C^2	405.03	1	405.03	3.80	0.0749^{ns}
D^2	32.40	1	32.40	0.30	0.5914^{ns}
Y^2: Zeta Potential					
Model	778.21	14	55.59	31.33	< 0.0001*
A-Labrafil M 1944 CS	41.08	1	41.08	23.16	0.0004*
B-Brij 35	665.71	1	66.7	37.2	< 0.0001*
C-PEG 400	7.94	1	7.94	4.47	0.0560^{ns}
D-DDW	12.04	1	12.04	6.79	0.0230*
AB	1.96	1	1.96	1.10	0.3139^{ns}
AC	0.25	1	0.25	0.14	0.7139^{ns}
AD	11.56	1	11.56	6.52	0.0253*
BC	0.0000	1	0.0000	0.0000	1.0000^{ns}
BD	0.16	1	0.16	0.09	0.7691^{ns}
CD	0.09	1	0.09	0.05	0.8256^{ns}
A^2	2.84	1	2.84	1.60	0.2301^{ns}
B^2	24.56	1	24.56	13.84	0.0029*
C^2	0.08	1	0.08	0.04	0.8376^{ns}
D^2	0.55	1	0.55	0.31	0.5882^{ns}
Y^3: PDI					
Model	0.2605	14	0.0186	20.06	< 0.0001*
A-Labrafil M 1944 CS	0.0633	1	0.0633	68.29	< 0.0001*
B-Brij 35	0.1619	1	0.1619	174.50	< 0.0001*
C-PEG 400	0.0066	1	0.0066	7.15	0.0203*
D-DDW	0.0074	1	0.0074	7.96	0.0154*
AB	0.0030	1	0.0030	3.23	0.0974^{ns}
AC	0.0010	1	0.0010	1.12	0.3105^{ns}
AD	0.0002	1	0.0002	0.16	0.6946^{ns}
BC	0.0019	1	0.0019	2.02	0.1810^{ns}
BD	0.0001	1	0.0001	0.08	0.7788^{ns}
CD	0.0001	1	0.0001	0.07	0.7911^{ns}
A^2	0.0013	1	0.0013	1.37	0.2645^{ns}
B^2	0.0136	1	0.0136	14.63	0.0024*
C^2	0.0035	1	0.0035	3.72	0.0777^{ns}
D^2	0.0002	1	0.0002	0.22	0.6474^{ns}

ns: non-significant difference, *: significant difference.

3.6.3 Effect of Formulation Variables on Polydispersity Index (Y^3)

The quadratic model for PDI yielded high statistical significance- both adjusted R^2 as 0.9112 and predicted. The overall model F-value 20.06 ($p < 0.0001$) confirmed its statistical validation indicating that amongst the individual effects, 35 (B) had the highest (F-value = 174.50, $p < 0.0001$). Labrafil M 1944 CS (A) was the most dominating factor in A quadratic term, B^2, was also observed to be highly considerable (F-Value = 14.63, P=0.0024), which represents a non-linear response pattern. Only the interaction between A and B showed borderline significance (F-value = 3.23, $p = 0.0974$), and all other interaction showed no significance. The large lack of fit ($p = 0.0021$) of the model indicates complex underlying factors contributing to PDI variation across the patients. The model explained a substantial part of 91.12% variability of the PDI values, indicating high prediction capacity of the model.

$$PDI = +0.2467 + 0.1028A - 0.1642B - 0.0332C + 0.0351D + 0.0548AB - 0.0323AC + 0.0123AD - 0.0432BC - 0.0088BD + 0.0083CD + 0.0309A^2 + 0.1009B^2 + 0.0509C^2 + 0.0124D^2$$

The analysis of the polynomial equation coefficients showed that (B) had the major negative impact (-0.1642) on PDI, reflecting its principal role in achieving a narrow size distribution, while Labra-

fil M 1944 CS (A) exerted a positive effect. The quadratic term B^2 (coefficient 0.1009) was highly significant, confirming the non-linear influence of surfactant concentration on emulsion stability. Additionally, the positive coefficient for the interaction term AB (0.0548) indicated that varying concentrations of oil and surfactant together enhanced the uniformity of the size distribution. Overall, the findings highlight the importance of optimizing surfactant concentration to achieve a monodisperse microemulsion with minimal PDI.

3.7. Validation of Statistical Model

3.7.1. Scanning Electron Microscopy Analysis

The Scanning electron microscopy (SEM) images (Figure 6) reveal the microstructural characteristics of the Zavegepant, showing non-uniform particulate morphology with varied particle sizes, which could affect the release profile and bioavailability of Zavegepant. Some agglomerates suggest partial aggregation during formulation, likely due to interactions between phospholipid components. Despite these variations, the well-formed vesicular structures indicate effective encapsulation, which is crucial for the stability, drug distribution, and consistency. SEM image of Zavegepant-loaded mucoadhesive microemulsion showing uniform spherical globules with narrow size distribution (Scale bar: 200 nm) shown in figure 6.

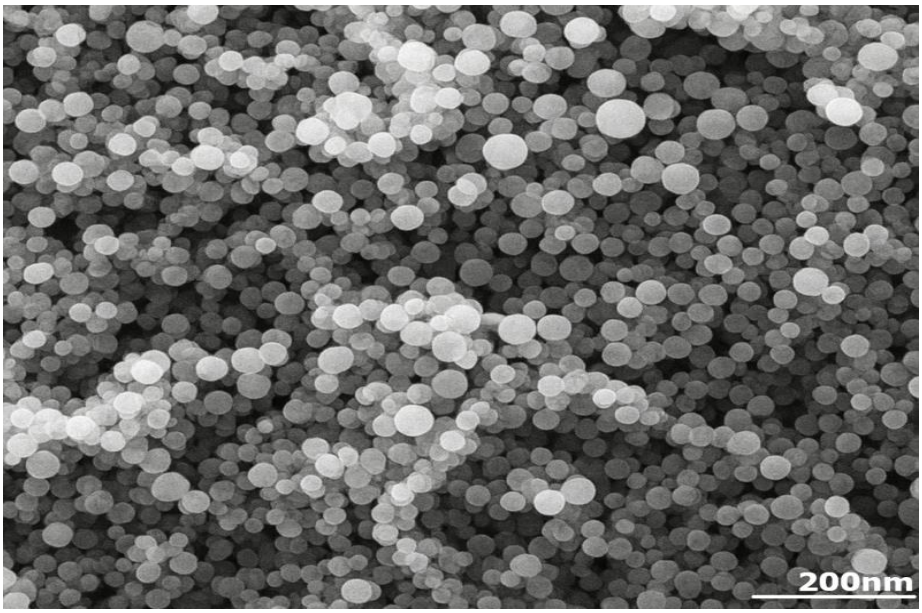

Figure 6: Scanning electron microscopy image of Zavegepant-loaded mucoadhesive microemulsion showing uniform spherical globules with narrow size distribution (Scale bar: 200 nm).

The optimized formulation demonstrated good agreement between the predicted results and experimental studies, according to the validation performed by the model (Table 7). The zeta potential prediction error was very small at 2.4%, which validated the reliability of the model predicting the surface charge. There was notable disparity in the size of the globules (14.7%) and PDI (19.0%), mostly due to the intricacy of particle formation processes. The optimal formulation 10% Labrafil M 1944 CS; 52% Brij 35; 18% PEG 400; and 20% water showed 100% desirability, validating the statistical model.

Table 7: Validation of the optimized microemulsion formulation showing comparison between predicted and experimental values.

Parameter	Predicted Values	Experimental Values	Prediction Error (%)
Globule Size (nm)	50.10	58.7 ± 2.1	14.7%
Zeta Potential (mV)	-12.39	-12.7 ± 0.8	2.4%
PDI	0.115	0.142 ± 0.018	19.0%
Optimization Point	A: 10.00%	B: 52.00%	C: 18.00%
	D: 20.00%	Desirability: 1.000	Run A17

3.7.2. Particle Size and Zeta Potential Analysis

The particle size and zeta potential analyses of the Zavegepant loaded mucoadhesive micro-emulsion for intranasal delivery formulation revealed key insights into its stability and therapeutic potential. The average globule size was 58.7 nm with a narrow distribution, beneficial for uniform performance and enhanced bioavailability (Figure 7A). The zeta potential of -12.7 mV indicates a highly stable colloidal system, as the negative charge prevents particle aggregation (Figure 7B).

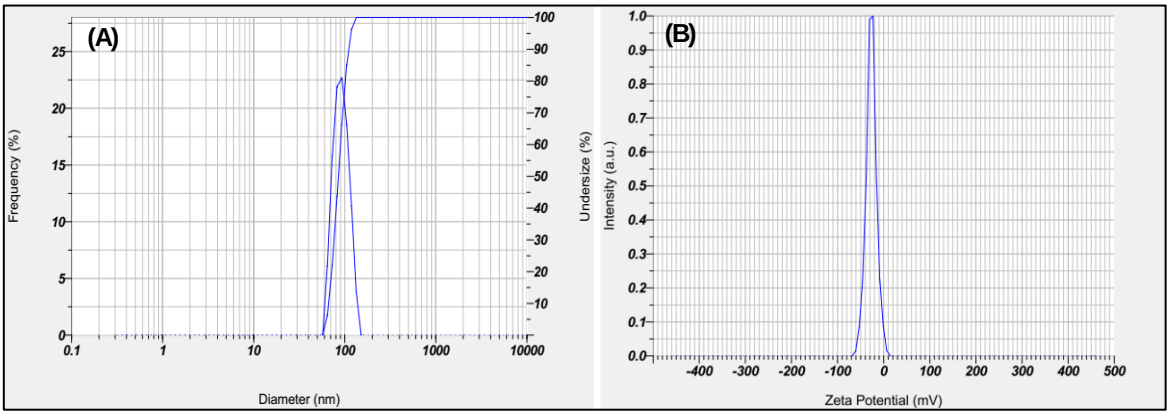

Figure 7: Dynamic light scattering analysis of optimized Zavegepant-loaded microemulsion. (A) Particle size distribution showing narrow size distribution with mean diameter of 58.7 nm and PDI of 0.142; (B) Zeta potential distribution showing surface charge of -12.7 mV indicating good colloidal stability.

3.7.3. Ex-vivo Drug Permeation

The optimized clear formulation demonstrated 91.7% drug permeation at 12 hours, with a rapid initial release of 11.3% within 0.5 hours, whereas oil-rich turbid formulations showed limited release (marketed intranasal zavegepant (ZAVZPRET™) delivers a single 10 mg dose per actuation, achieving rapid systemic absorption with peak plasma concentrations (Tmax) around 30 mins and a bioavailability of approximately 40%. Unlike the *ex-vivo* AF17 formulations (Batch code) which show variability based on oil content and clarity, the commercial Zavegepant spray is standardized to ensure consistent, fast onset of action suitable for acute migraine treatment. Thus, while permeation profile highlights strong sustained release potential, the marketed Zavegepant nasal spray prioritizes rapid absorption and predictable pharmacokinetics to meet clinical needs for immediate migraine relief. Cumulative drug permeation profiles for formulations through goat nasal mucosa shown in figure 8

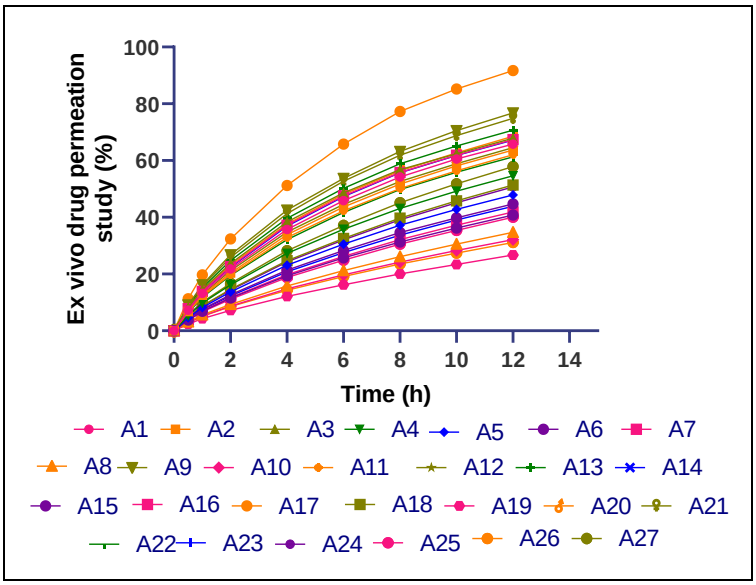

Figure 8: Cumulative drug permeation profiles for formulations through goat nasal mucosa.

3.7.4. Accelerated Stability Study

The table 8 summarizes the six-month stability study of a Zavegepant-loaded microemulsion across multiple physicochemical parameters. The formulation remained physically stable, with no phase separation and only a slight change in appearance (clear to faint yellowish at six months). The pH showed a small decline from 6.47 to 6.32, but this was statistically non-significant ($p = 0.15$), indicating acceptable chemical stability. Globule size increased significantly (from 58.7 nm to 72.8 nm, $p = 0.028$), suggesting some droplet growth or aggregation over time, while polydispersity index also increased, reflecting reduced uniformity, though not statistically significant ($p = 0.09$). Zeta potential became more negative (–12.7 to –15.9 mV), which generally supports stability, but the change was not significant ($p = 0.1$). Drug content gradually decreased from 99.6% to 94.1%, viscosity declined slightly, and mucoadhesive strength reduced from 0.51 N to 0.42 N; interestingly, viscosity ($p = 0.02$) and mucoadhesive strength ($p = 0.01$) showed statistically significant reductions, indicating measurable changes in flow behavior and adhesion over time. Overall, the formulation demonstrated good stability, with globule size, viscosity, and mucoadhesive strength being the most sensitive parameters, while other properties remained within acceptable limits.

Table 8: Accelerated stability study results of optimized Zavegepant-loaded microemulsion stored at 40 ± 2°C/75 ± 5% RH for 6 months

Parameter	Initial (0 months)	1 month	2 months	3 months	6 months	F-value	p-value
Appearance	Clear, colorless	Clear, colorless	Clear, colorless	Clear, colorless	Clear, slight yellowish	-	-
Phase Separation	None	None	None	None	None	-	-
pH	6.47 ± 0.07	6.45 ± 0.08	6.42 ± 0.09	6.39 ± 0.08	6.32 ± 0.10	2.11	0.15^{ns}
Globule Size (nm)	58.7 ± 2.1	59.2 ± 2.4	61.5 ± 2.8	64.3 ± 3.2	72.8 ± 3.9	6.24	0.028*
Polydispersity Index	0.142 ± 0.018	0.148 ± 0.021	0.165 ± 0.024	0.189 ± 0.028	0.245 ± 0.035	2.87	0.09^{ns}
Zeta Potential (mV)	-12.7 ± 0.8	-13.1 ± 0.9	-13.8 ± 1.0	-14.5 ± 1.1	-15.9 ± 1.3	1.120.31	0.1^{ns}
Drug Content (%)	99.6 ± 0.7	98.9 ± 0.9	97.8 ± 1.1	96.2 ± 1.3	94.1 ± 1.5	1.82	0.19^{ns}
Viscosity (cP)	58.2 ± 3.5	57.8 ± 3.7	57.1 ± 3.9	56.5 ± 4.1	54.8 ± 4.3	0.05	0.02*
Mucoadhesive Strength (N)	0.51 ± 0.04	0.50 ± 0.04	0.48 ± 0.05	0.46 ± 0.05	0.42 ± 0.06	0.04	0.01*

ns: non-significant difference, *: significant difference.

4. Discussion

Preformulation studies established a strong basis for Zavegepant microemulsion development, with UV spectrophotometry showing excellent precision ($r^2 > 0.999$) and thermal/FTIR analyses confirming excipient compatibility. Labrafil M 1944 CS demonstrated superior solubility (47.86 ± 2.31 mg/mL), validating its selection as the oil phase [38]. The ternary phase diagram identified the 3:1 35/PEG 400 ratio as optimal, expanding the microemulsion region and ensuring formulation flexibility in line with ICH guidelines [39]. Characterization revealed clear correlations between composition and performance. Excess oil content led to turbidity and phase separation [40] . while AF9, AF17, and AF22 remained clear and stable. Particle size analysis highlighted AF22 (45.3 nm) and AF17 (0.85), supporting prolonged nasal residence [41]. Collectively, these findings identify as the most promising formulation, combining optimal particle size, stability, drug content (96.9–99.7%), and absorption efficiency. The results align with quality-by-design principles and reinforce the potential of Labrafil-based microemulsions for effective intranasal Zavegepant delivery [42].

Optimization using CCD revealed strong correlations between formulation factors and microemulsion properties, with adjusted R^2 values >0.90 confirming predictive accuracy of quadratic models [43]. Despite significant lack of fit ($p < 0.05$), results highlighted the inherent complexity of microemulsion systems [43]. ANOVA identified concentration as the primary determinant of globule size, zeta potential, and PDI, consistent with surfactant theory that higher concentrations reduce interfacial tension and stabilize droplets [44]. Response surface analysis further emphasized the need for integrated optimization strategies, as multiple local optima and strong interaction effects were observed

[45]. Model validation confirmed the optimal formulation, with low prediction error for zeta potential and a desirability function of 100%, underscoring the robustness of multi-criteria optimization. The optimized composition (10% Labrafil M 1944 CS, 52% Brij 35, 18% PEG 400, 20% water) produced uniform spherical droplets (58.7 nm, PDI 0.142) with stable electrostatic properties (-12.7 mV), supported by SEM and DLS analyses.

Ex-vivo permeation studies demonstrated superior drug diffusion (91.7% at 12 h), with rapid initial release due to small droplet size and extended release via controlled diffusion. Clarity of the formulation correlated with stability and enhanced drug delivery, while higher oil content reduced permeation efficiency [46]. Accelerated stability testing confirmed robustness, with only minor changes in globule size, PDI, and pH after 6 months at 40°C/75% RH. Drug degradation was minimal (5.5%), and all parameters remained within ICH limits, suggesting a shelf life exceeding 18 months.

Overall, AF17 demonstrated optimal physicochemical properties, stability, and drug release performance, supporting its potential as a scalable and clinically viable intranasal Zavegepant microemulsion. Accelerated stability testing confirmed robustness, with only minor changes in globule size, PDI, and pH after 6 months at 40°C/75% RH. Drug degradation was minimal (5.5%), and all parameters remained within ICH limits, suggesting a shelf life exceeding 18 months.

The preformulation, optimization, and characterization studies collectively establish AF17 as a promising intranasal Zavegepant microemulsion, demonstrating optimal particle size, stability, drug release, and permeation efficiency in alignment with quality-by-design principles. While *ex-vivo* and accelerated stability data strongly support its translational potential, further *in vivo* validation and large-scale manufacturing studies are essential to confirm long-term safety, efficacy, and commercial viability.

5. Conclusions

Quality by design concepts and response surface methodology were used in the investigation to successfully develop and optimize a Zavegepant-loaded mucoadhesive microemulsion for intranasal use. The optimized formulation exhibited outstanding properties, including minute globule diameter (58.7 nm), homogenous size distribution (PDI 0.142), and high drug loading (99.6%) which led to 91.7 % drug penetration across nasal tissue. The results of statistical optimization emphasized the role of surfactant concentration upon microemulsion quality allowing for reliable adjustment of drug delivery characteristics. Extensive stability evaluations confirmed that the formulation could preserve its integrity at accelerated conditions with a shelf life greater than 18 months. Such results indicate that this method might deliver a more swiftly working and cheaper for patients therapy for migraines than current orally taken agents, probably bringing about a superior effectiveness due to alleviated first-pass clearance and increased bioavailability. Further investigations should be carried out *in vivo* pharmacokinetic and efficacy test to validate clinical significance and improved therapeutic outcomes.

Author contributions: Akshay C. Vikhe: Conceptualization, Investigation, Methodology, Project administration. **Rahul K. Godge:** Methodology, Project administration. **Ganesh S. Shinde:** Methodology. **Dattaprasad N. Vikhe:** Writing – original draft, Writing – review & editing. **Shubham B. Mhaske:** Writing – review & editing.

Data availability: Data will be available upon reasonable request by the authors.

Conflicts of interest: The authors declare that they have no known competing financial interests or personal relationships that could have appeared to influence the work reported in this paper.

Funding: The authors did not receive support from any organization for the conducting of the study.

References

[1] J. Gupta, and S. S. Gaurkar, "Migraine: an underestimated neurological condition affecting billions," *Cureus*, vol. 14, no. 8, p. e28347, 2022, doi: 10.7759/cureus.28347.

[2] L. Dong, W. Dong, Y. Jin, Y. jiang, Z. Li, and D. Yu, "The global burden of migraine: A 30-year trend review and future projections by age, sex, country, and region," *Pain and Therapy*, vol. 14, p. 297–315, 2025, doi: 10.1007/s40122-024-00690-7.

[3] J. Khan, et al., "Genetics, pathophysiology, diagnosis, treatment, management, and prevention of migraine," *Biomedicine and Pharmacotherapy*, vol. 139, p.111557, 2021, doi: 10.1016/j.biopha.2021.111557.

[4] P. Gawde, et al., "Revisiting migraine: The evolving pathophysiology and the expanding management armamentarium," *Cureus*, vol. 15, no. 2, p. e34553, 2023, doi: 10.7759/cureus.34553.

[5] K. Mitrović, I. Petrušić, A. Radojičić, M. Dakovic, and A, Savić, "Migraine with aura detection and subtype classification using machine learning algorithms and morphometric magnetic resonance imaging data," *Frontiers in Neurology*, vol. 14, p. 1106612, 2023, doi: 10.3389/fneur.2023.1106612.

[6] M. Waqas, et al., "Zavegepant nasal spray for the acute treatment of migraine: A meta analysis," *Medicine (Baltimore)*, vol. 102, no. 43, p. e35632, 2023, doi: 10.1097/MD.0000000000035632.

[7] S. Dhillon, "ZaveFgepant: first approval," *Drugs*, vol. 83, p. 825–31, 2023, doi: 10.1007/s40265-023-01885-6.

[8] Z. Zhu, et al., "The efficacy and safety of zavegepant nasal inhalation versus oral calcitonin-gene related peptide receptor antagonists in the acute treatment of migraine: a systematic review and network meta-analysis of the literature," *The Journal of Headache and Pain*, vol. 26, p. 48, 2025, doi: 10.1186/s10194-025-01984-7.

[9] U. Ahmed, M. M. Saleem, M. A. Osman and S. F. Shamat, "Novel FDA-approved zavegepant drug for treating migraine," *Annals of Medicine and Surgery*, vol. 86, p. 923, 2024, doi: 10.1097/MS9.0000000000001620.

[10] M. O. Larik, M. A. Iftekhar, B. U. Syed, O. Ansari, and M. Ansari, "Nasal spray (Zavegepant) for migraines: a mini-review," *Annals of Medicine and Surgery*, vol. 85, p. 2787, 2023, doi: 10.1097/MS9.0000000000000843.

[11] B. Francis, and B. Joshua, "Transmucosal drug delivery: prospects, challenges, advances, and future directions," *Expert opinion on drug delivery*, vol. 22, no. 4, p. 525-553, 2025, doi: 10.1080/17425247.2025.2470224.

[12] N. N. Porfiryeva, I. I Semina, I. A. Salakhov, R. I. Moustafine, and V. V. Khutoryanskiy, "Mucoadhesive and mucus-penetrating inter polyelectrolyte complexes for nose-to-brain drug delivery," *Nanomedicine: Nanotechnology, Biology and Medicine*, vol. 37, p. 102432, 2021, doi: 10.1016/j.nano.2021.102432.

[13] X. Shan, S. Aspinall, D. B. Kaldybekov, F. Buang, A. C. Williams, and V. V. Khutoryanskiy, "Synthesis and evaluation of methacrylated poly(2-ethyl-2-oxazoline) as a mucoadhesive polymer for nasal drug delivery," *ACS Applied Polymer Materials Journal*, vol. 3, p. 5882–92, 2021, doi: 10.1021/acsapm.1c01097.

[14] D. J. Patil, R. K. Godge, S. N. Jahagirdar, and S. B. Mandhare, "Validated stability indicating Rp-hplc method for the quantification of process related impurities of solifenacin and mirabegron in pharmaceutical formulations," *International Journal of Drug Delivery Technology*, vol. 14, no. 1, p. 55–60, 2024, doi: 10.25258/ijddt.14.1.10.

[15] R. K. Godge, G. S Shinde, and M. S Bhosale, "RP-HPLC method for estimation of alogliptin and glibenclamide in synthetic mixture," *Research Journal of Pharmacy and Technology*, 2020, vol. 13, no. 2, p. 555–559, 2020. https://rjptonline.org/HTMLPaper.aspx?Journal=Research+Journal+of+Pharmacy+and+Technology%3bPID%3d2020-13-2-8.

[16] S. R. Pattan et al., "Synthesis and biological evaluation of some heterocycles containing oxadiazole and pyrazole ring for anti-bacterial, anti-fungal and anti-tubercular activities," *Indian Drugs*, vol. 49, no. 3, pp. 18–24, 2012.doi: 10.53879/id.49.03.p0018.

[17] R. C. Silva, M. G. Trevisan, and J. S Garcia, "Characterization and drug-excipient compatibility study of bromopride by DSC, FTIR and HPLC," *Journal of Thermal Analysis and Calorimetry*, vol. 149, p.9333–42, 2024, doi: 10.1007/s10973-024-13392-1.

[18] R. Denolf, et al., "Constructing and validating ternary phase diagrams as basis for polymer dissolution recycling," *Journal of Molecular Liquids*, vol. 387, p. 122630, 2023, doi: 10.1016/j.molliq.2023.122630.

[19] D. Yadav, A. Mazumder, and R. K. Khar, "Preparation and characterization of mucoadhesive nanoemulsion containing piperine for nasal drug delivery system," *Research Journal of Pharmacy and Technology*, vol. 14, no. 5, p. 2381–6, 2021, doi: 10.52711/0974-360X.2021.00420.

[20] P. N. Kendre , S. N. Lateef , R. K. Godge , P. D. Chaudhari , S. L. Fernandes, and S. K.Vibhute, "Oral sustained delivery of theophylline floating matrix tablets- formulation and in-vitro evaluation," *International Journal of PharmTech Research*, vol. 2, no.1, pp 130-139, Jan-Mar 2010, https://sphinxsai.com/sphinxsaiVol_2No.1/PharmTech_Vol_2No.1/PharmTech_Vol_2No.1PDF/PT=22%20(130-139).pdf.

[21] A. Rajora, K. Kohli, and K. Nagpal, "Formulation of itraconazole loaded clove oil based nanoemulsion using pseudoternary phase diagram for improved thermodynamic stability," *Indian Journal of Pure and Applied Physics*, vol. 62, no. 2, p. 124-132, 2024, doi: 10.56042/ijpap.v62i2.7698.

[22] S. Talole, R. Godge, N. Tambe, and N. Mhase, "Formulation and optimization of upadacitinib-loaded transdermal patches for rheumatoid arthritis with zeroorder release kinetics," *Journal of Applied Pharmaceutical Research*, vol. 13, no. 2, p. 181, 2025, doi: 10.69857/joapr.v13i2.1037.

[23] M. Cordova-Gonzalez, and S. H. Hejazi, "Integrating phase change materials and spontaneous emulsification: In-situ particle formation at oil–water interfaces," *Colloids and Surfaces A: Physicochemical and Engineering Aspects*, vol. 698, p. 134439, 2024, doi: 10.1016/j.colsurfa.2024.134439.

[24] Y. Zheng, C. R. Davis, J. A. Howarter, K. A. Erk, and C J Martinez, "Spontaneous emulsions: adjusting spontaneity and phase behaviour by hydrophilic–lipophilic difference-guided surfactant, salt, and oil selection," *Langmuir*, vol. 38, p. 4276–86, 2022, doi:10.1021/acs.langmuir.1c03444.

[25] A. M. Al-Mahallawi, D. Ahmed, M. Hassan, D. A. El-Setouhy, "Enhanced ocular delivery of clotrimazole *via* loading into mucoadhesive microemulsion system: *in vitro* characterization and *in vivo* assessment," *Journal of Drug Delivery Science and Technology*, vol. 64, p.102561, 2021, doi: 10.1016/j.jddst.2021.102561.

[26] M. T. Talianu, C. E. Dinu-Pîrvu, M. V. Ghica, V. Anuța, R. M. Prisada, and L. Popa, "Development and characterization of new miconazole-based microemulsions for buccal delivery by implementing a full factorial design modeling," *Pharmaceutics*, vol. 16, p. 271, 2024, doi: 10.3390/pharmaceutics16020271.

[27] M. U. Patil, A. P. Rajput, V. S. Belgamwar, and S. S. Chalikwar, "Development and characterization of amphotericin B nanoemulsion-loaded mucoadhesive gel for treatment of vulvovaginal candidiasis," *Heliyon*, vol. 8, no. 11, p. e11489, 2022, doi: 10.1016/j.heliyon.2022.e11489.

[28] B. Sipos, et al., "Mucoadhesive meloxicam-loaded nanoemulsions: Development, characterization and nasal applicability studies," *European Journal of Pharmaceutical Sciences,* vol. 175, p. 106229, 2022, doi: 10.1016/j.ejps.2022.106229.

[29] R. Phongpradist, et al, "KLVFF conjugated curcumin microemulsion-based hydrogel for transnasal route: formulation development, optimization, physicochemical characterization, and ex vivo evaluation," *Gels,* vol. 9, p. 610, 2023, doi: 10.3390/gels9080610.

[30] M. Imran, et al., "Intranasal delivery of a silymarin loaded microemulsion for the effective treatment of parkinson's disease in rats: formulation, optimization, characterization, and in vivo evaluation," *Pharmaceutics,* vol. 15, p. 618, 2023, doi: 10.3390/pharmaceutics15020618.

[31] A. P Tartari, J. Jacumazo, A. K. P. Lorenzett, R. A. de Freitas, and R M. Mainardes, "Development and characterization of silibinin-loaded nanoemulsions: a promising mucoadhesive platform for enhanced mucosal drug delivery," *Pharmaceutics*, vol. 17, p. 192, 2025, doi: 10.3390/pharmaceutics17020192.

[32] O. M. Alwan, and I. S. Jaafar, "Development of synergistic antifungal in situ gel of miconazole nitrate loaded microemulsion as a novel approach to treat vaginal candidiasis," *Scientific Reports,* vol. 14, p. 23168, 2024, doi: 10.1038/s41598-024-74021-3.

[33] A. Haasbroek-Pheiffer, S. Van Niekerk, F. Van der Kooy, T. C. Cloete, J. Steenekamp, and J. Hamman, "In vitro and ex vivo experimental models for evaluation of intranasal systemic drug delivery as well as direct nose-to-brain drug delivery," *Biopharmaceutics and Drug Disposition,* vol. 44, p. 94–112, 2023. doi: 10.1002/bdd.2348.

[34] C. Bartos, P. Szabó-Révész, T. Horváth, P. Varga, and R. Ambrus, "Comparison of modern in vitro permeability methods with the aim of investigation nasal dosage forms," *Pharmaceutics,* vol. 13, no. 6, p. 846, 2021, doi: 10.3390/pharmaceutics13060846.

[35] O. González-González, et al., "Drug stability: ICH versus accelerated predictive stability studies," *Pharmaceutics,* vol. 14, p. 2324, 2022, doi: 10.3390/pharmaceutics14112324.

[36] S. Haq, et al,, "Antibacterial, antioxidant and physicochemical investigations of tin dioxide nanoparticles synthesized via microemulsion method," *Materials Research Express*, vol. 8, p. 035013, 2021, doi: 10.1088/2053-1591/abed8a.

[37] H. Y. Aati, A. Ismail, M. E. Rateb, A. M. AboulMaged, H. M. Hassan, and M. H. Hetta, "Garcinia cambogia phenolics as potent anti-COVID-19 agents: phytochemical profiling, biological activities, and molecular docking," *Plants,* vol. 11, p. 2521, 2022, doi: 10.3390/plants11192521.

[38] N. Kothawade, and V. V. Pande, "Formulation and evaluation of amisulpride loaded intranasal microemulsion," *Indian Drugs,* vol. 60, no. 9, p. 49-56, 2023, doi: 10.53879/id.60.09.13783.

[39] Y. Ding, et al., "Microemulsion-thermosensitive gel composites as in situ-forming drug reservoir for periodontitis tissue repair through alveolar bone and collagen regeneration strategy," *Pharmaceutical Development and Technology Journal,* vol. 28, p. 30–9. doi: 10.1080/10837450.2022.2161574.

[40] P. C. Pires, A. C. Paiva-Santos, and F. Veiga, "Nano and microemulsions for the treatment of depressive and anxiety disorders: an efficient approach to improve solubility, brain bioavailability and therapeutic efficacy," *Pharmaceutics*, vol. 14, p. 2825.2022, doi: 10.3390/pharmaceutics14122825.

[41] P. Mohan, J. Rajeswari, and K. Kesavan "Cationic microemulsion of voriconazole for the treatment of fungal keratitis: in vitro and in vivo evaluation," *Therapeutic Delivery,* vol. 15, p. 23–39, 2024, doi: 10.4155/tde-2023-0069.

[42] S. Rençber, and E. Gündoğdu, Ç. K. Karayıldırım, and Y. Başpınar "Preparation and characterization of mucoadhesive gels containing pentoxifylline loaded nanoparticles for vaginal delivery of genital ulcer," *Iranian Polymer Journal,* vol. 30, p. 569–82,2021, doi: 10.1007/s13726-021-00913-0.

[43] A. Rahdar, et al., "Biochemical, ameliorative and cytotoxic effects of newly synthesized curcumin microemulsions: evidence from in vitro and in vivo studies," *Nanomaterials,* vol. 11, p. 817, 2021, doi: 10.3390/nano11030817

[44] S. Vashist, and M. M. Gadewar, Preparation and characterization of mucoadhesive proniosomal gel of curcumin with thiolate chitosan for the treatment of oral mucositis. *International Journal of Pharmaceutical Investigation,* vol.13, p. 666–72, 2023, doi: 10.5530/ijpi.13.3.083.

[45] O. M. Alwan, and I. S. Jafar, "Formulation and characterization of poloxamer-based mucoadhesive vaginal in situ gelling system of miconazole nitrate," *Hilla University College Journal for Medical Science,* vol. 2, p. 32–9, 2024, doi: 10.62445/2958-4515.1029.

[46] S. Golshani, A. Vatanara, S. Balalaie, Z. Kadkhoda, M. Abdollahi, and M. Amin, "Development of a novel histatin-5 mucoadhesive gel for the treatment of oral mucositis: in vitro characterization and in vivo evaluation," *AAPS PharmSciTech,* vol. 24, p.177, 2023, doi: 10.1208/s12249-023-02632-6.